

SIZE DISTRIBUTION IN GROWTH OF FINE PARTICLES

Vladimir Privman

Department of Physics, Clarkson University
Potsdam, New York 13699–5820, USA

Electronic mail: privman@clarkson.edu

ABSTRACT

We review recent theoretical work on predicting size distribution in synthesis of narrow-size-distribution particles of colloidal dimensions, when the mechanism of size selection involves a combination of two growth/aggregation processes. Nuclei, produced rapidly in a supersaturated solution, grow to nanosize primary particles, which then aggregate to form much larger final (secondary) particles. Our kinetic model explains the formation of dispersions of narrow size distribution in such processes. Numerical simulations of the kinetic equations, with experimental model parameter values, yield results that agree semiquantitatively with experimental observations.

1. INTRODUCTION

This short review presents the recently developed theoretical model [1] of growth of monodispersed colloids by precipitation from homogeneous solutions [2-8]. Systematic experimental studies of the mechanisms of synthesis and properties of monodispersed colloids have been initiated about quarter a century ago. A large number of dispersions of uniform particles of various chemical composition and shape, ranging in size from fraction of a micron to few microns, have been described. Theoretical description of the formation of uniform colloids relies on experimental identification of solute species that are involved in the various stages of the particle formation and on observation of growth stages leading from the initial nucleation to final particles. Early theoretical modeling was based on the mechanism suggested by LaMer: a short nucleation burst, followed by diffusional growth of the resulting nuclei to form identical fine particles [8,9].

However, there has been mounting experimental evidence that the burst-nucleation/diffusional growth mechanism alone is inadequate. Specifically, it has been found that many spherical particles precipitated from solution showed polycrystalline X-ray characteristics, such as ZnS [10], CdS [11], Fe_2O_3 [12], etc. These particles are not single crystals. Rather, it has been confirmed by several techniques (small angle light scattering, electron microscopy, X-ray diffraction) that most monodispersed colloids consist of small crystalline subunits [10-20]. Furthermore, it has been observed [1,7,16] that the crystalline subunits in the final particles were of the same size as the diameter of the precursor-subunit “singlets” formed in solution, thus suggesting an aggregation-of-subunits mechanism. The two-stage growth process is shown schematically in Figure 1.

The substructures have been identified also in particles of shapes differ-

ent from spherical, and it has been recognized that different morphologies of the final particles must be related to the nature of the precursor singlets [12,18-20]. This experimental evidence has led to two major theoretical challenges. First, the morphology and shape selection of particles formed by interplay of nucleation and aggregation processes must be explained. Second, the size-selection mechanism, i.e., the kinetics of generation of narrow particle size distribution, must be identified. Several theoretical approaches utilizing thermodynamic and dynamical growth mechanisms [1,4,5,18,21-32] have been described in the literature. Models of aggregation of subunits can be developed that yield a peaked and even sharpening with time particle size distribution [21-34]. However, none of the earlier attempts could fit quantitatively a broad range of experimental findings. Here we review the first results of a new approach [1] that explains the *size selection*, by coupling the dynamical equations for the processes of secondary particle growth by aggregation of subunits and of formation (nucleation) of these subunits.

Thus, the main new finding of our work [1], crucial to obtaining narrow size distribution, has been that the growth of the final, secondary particles by aggregation of singlets, must be coupled, via the rate of formation of these primary particles (singlets), to the time-dependence of the process of their nucleation and growth. We take the simplest possible models of both processes (primary and secondary particle formation). This choice simplifies numerical simulations and thus allows to scan a wider range of parameters. It avoids introduction of unknown microscopic parameters; as a result we only fit *one* parameter, the effective surface tension, and even that parameter turns out to be close to the experimental bulk value. This review is organized as follows. In Section 2, a kinetic model of secondary particle formation by singlet-capture dominated growth is considered. In Section 3, primary particle (singlet) formation by burst nucleation is de-

scribed. Finally, Section 4 reports results of numerical simulations and comparison with an experiment.

2. GROWTH OF THE SECONDARY PARTICLES

In colloid particle synthesis of the type considered here, in the initial induction step solutes are formed to yield a supersaturated solution, leading to nucleation; see Figure 1. The nuclei might then further grow by a diffusive mechanism. The resulting primary particles (singlets) in turn aggregate to form secondary particles. The latter process, to be modeled in this section, is facilitated by the appropriate chemical conditions in the system: the ionic strength and/or pH must assume values such that the surface potential approaches the isoelectric point, resulting in reduction of electrostatic barriers, thus promoting particle aggregation. Formation of the final (secondary) particles, which can be of narrow size distribution, is clearly a diffusion-controlled process [1-7].

An important experimental observation is that secondary particles are sufficiently sparsely positioned in solution to consider their evolution as largely independent. Furthermore, we will assume that the particles are spherical, with density close to that of the bulk material, which is experimentally a very common case, and the focus will be on their size distribution due to growth by aggregation, essentially, by consumption of diffusing singlets (monomers, primary particles). Several other simplifying assumptions will be made in order to zero-in on the essential ingredients of the theoretical modeling and make numerical simulations tractable. Thus, we do not address the processes by which the singlets forming secondary particles undergo restructuring and rearrangements resulting in compact structures and leading to shape selection. Some of the approximations made will be discussed at the end of this section. We focus on the two main stages in the process: the production of the primary and secondary particles; see Figure 1. The latter will be treated presently, while the formation of nuclei

and their possible growth (aging) to primary particles will be considered in the next section.

Kinetic rate-equation models of aggregation typically utilize a master equation for the distribution of growing particles by their size. Here the size will be defined by how many primary particles (singlets) were aggregated into each secondary particle, denoted by $s = 1, 2, \dots$. The growing particles can adsorb or emit singlets and multiplets. The master equation is then quite standard to set up, as in, e.g., [33]. In the present case, the process is experimentally documented to be highly irreversible, so that detachment can be disregarded. By considering the number of singlets, s , as the only parameter characterizing the cluster, we use the approximation that assumes that internal relaxation/restructuring processes within the cluster (growing secondary particle) are fast, and that they result in an approximately spherical object, of density similar to that of the bulk material, so that the voids have been largely eliminated and the solvent pushed out in the internal restructuring. We will comment on this point again later.

Furthermore, it is assumed that the singlets have diffusion constants larger than aggregates so that their capture dominates the growth process; this approximation will be also discussed again, shortly. The master equation then takes the form

$$\frac{dN_s}{dt} = w_{s-1}N_{s-1} - w_s N_s \quad (s > 1). \quad (1)$$

Here $N_s(t)$ is the time-dependent number density (per unit volume) of the secondary particles consisting of s primary particles. The attachment rate w_s will be taken from Smoluchowski's expression [35],

$$w_s(t) = 4\pi R_s D N_1(t), \quad (2)$$

where R_s is the radius of the s -singlet particle, given by

$$R_s = 1.2 r s^{1/3}. \quad (3)$$

The parameters r , the primary particle radius, and D , their diffusion constant, are experimentally available. The constant 1.2 in equation (3) was calculated as

$$(0.58)^{-1/3} \simeq 1.2, \quad (4)$$

where 0.58 is the typical filling factor of the random loose packing of spheres [36]. The fact that all the primary particles were assumed to have the same radius r will be further commented on later. Note that the rate in equation (2) involves the product $R_s D \propto r D$, which, according to the Einstein formula for the diffusion constant, is not sensitive to the distribution of values of the radii r .

We note that this approach already involves various assumptions. For example, equation (2) corresponds to the attachment process that is fully irreversible. Furthermore, the above equations are only valid for large s . Indeed, in reality clusters of all sizes s and S can coagulate to form larger clusters of size $s + S$. These are produced with the rate $4\pi(R_s + R_S)(D_s + D_S)N_s N_S$ within the Smoluchowski approach, where for $s = S$ there is an additional factor of 1/2 owing to double-counting. Our ignoring all but the singlet capture processes, $S = 1$, is supported by the experimental observations but constitutes an approximation. Furthermore, the form (2) is only correct for $s \gg S = 1$. Thus, we used the above relations as shown simply to avoid introducing additional parameters. For instance, for $s = 1$, this amounted to ignoring the “double counting” factor of 1/2, and the added factor of 4 due to the radii and diffusion constants of the two singlets

adding up.

The evolution of the population of singlets, which is not covered by equation (1), is obtained from the conservation of matter,

$$N_1(t) + \sum_{j=2}^{\infty} j N_j(t) = N_1(0), \quad (5)$$

which assumes that initially, at time $t = 0$, there are only singlets. When combined with the assumption of the singlet-capture dominance, the particle distribution is confined to small sizes, as has been confirmed by numerical simulations and other studies [1,37]. Indeed, most singlets will simply combine into dimers, fewer trimers, etc., and then the growth stops. The conventional approach has been to consider more general models, with discrete or continuous population balance, restoring multiplet aggregation, etc., which adds terms in and modifies the master equation (1); see, e.g., [21-34]. Typically such models have yielded wide size distributions [33,38-40].

We have developed [1] a new approach based on the observation that the supply of singlets is in itself a dynamical process. Numerical simulations indicate that if the concentration of the singlets were constant, i.e., if they were continuously generated to compensate for their depletion due to aggregation, then the resulting particle size distribution would be wide and peaked at small sizes, such that $N_s \simeq N_1 s^{-1/3}$ for sizes up to some growing cut-off s -value. However, if the supply of singlets is controlled in such a way that their concentration is a decaying function of time, then size selection can be obtained with some time-dependence protocols. For example, when the rate $\rho(t)$ at which the primary particles are formed (per unit volume) was chosen to be a decaying power-law, then numerical calculations [1] yielded a single-hump size distribution for the secondary particles. Note

that the equation for $N_1(t)$ must be modified by replacing relation (5) by

$$N_1(t) = \int_0^t \rho(t') dt' - \sum_{j=2}^{\infty} j N_j(t), \quad (6)$$

with the initial values $N_s(0) = 0$ for all $s = 1, 2, 3, \dots$

Equations of this type, with singlet-capture dominance of the dynamics and several ad hoc singlet-input rate functions, have been described in the literature [37]. The emphasis [37] has been on cases which are exactly solvable, e.g., one-dimensional versions, and those where the size distribution shows self-similar behavior. Our approach is quite different in that we actually *model* the primary-particle input rate $\rho(t)$ by using the burst-nucleation approach; see the next section.

Let us now further comment on the approximations involved in using the simplest kinetic equations for the aggregation process. These include, for instance, ignoring multiplet mobility and multiplet-multiplet collisions, as well as the effect of mobility of aggregates (multiplets) on the diffusion constants used in the rate expressions, etc., especially in the beginning of the process when most aggregates are small. There are established methods in the literature that avoid some of such difficulties [21-34] and, in fact, several of the models for various reaction rates lead to particle-size distributions peaked and even sharpening with time [22,34,42,43]. However, the main point of our work, which we believe is new and crucial to obtaining narrow size distributions, has been that the growth of the secondary particles must be coupled, via the rate of generation of singlets (primary particles), to the time-dependence of the process of formation of the latter; see the following sections.

Thus, we intentionally took the *simplest possible* models of both processes, the primary and secondary particle formation. This choice has the

following advantages: it simplifies numerical simulations and thus allows to scan a wider range of model parameters; it avoids introduction of unknown microscopic parameters. As a result, for instance, our description of the aggregation process in this section has *no adjustable parameters*; they are all experimentally available. Similarly in the following sections, for primary particle formation, we only utilize *one adjustable parameter*, the effective surface tension, and even that parameter turns out to be close to the experimental bulk value.

However, we recognize that more sophisticated modeling can improve consistency with experiment, perhaps at the expense of additional assumptions and parameters, and we intend to explore this avenue of investigation in future studies. In fact, we carried out preliminary numerical simulations allowing for the dimer diffusion and attachment to larger aggregates and showing trend of improved consistency with experiment. We furthermore note that the approximation of restricting the aggregation process to only the smallest particles sticking to larger particles has been already used in the literature, e.g., [22,27]. Considerations of colloid stability have been typically utilized to justify such approximations, and we note that detailed arguments of this sort would require additional microscopic parameters in the model.

We also comment that generally in diffusion limited growth the aggregates are expected to be fractal [38-41]. In this work we avoid the issue of shape selection and internal structure of the secondary particles; see review [21]. There are processes of internal rearrangement and pushing out of the solvent, going on during the secondary particle growth for typical experimental conditions, because the particles are clearly spherical throughout the growth process. In some experiments [14], the surface of the secondary particles was initially “hairy” and it got smoother at later times. We have

assumed that the internal rearrangement processes are fast enough so that the shape and morphology of the aggregates are, respectively, spherical and compact. One could propose that the effects of internal rearrangements in our model make the numerical coefficient, 1.2, in equation (3) another fit parameter rather than a fixed number. Distribution of the primary particle radii could also affect the porosity properties and thus modify this coefficient; we have not explored this matter.

3. NUCLEATION OF THE PRIMARY PARTICLES

In this section we evaluate the primary-particle production rate, $\rho(t)$, assuming fast nucleation [8,9,34,44]. Thermodynamic models of “burst” nucleation have been originally formulated in [8,9]. Modeling the rate of formation of primary particles (singlets) requires setting up a master equation, where the rate of growth is determined by the Boltzmann factor with the thermodynamic free energy difference ΔG , multiplied by $-1/(kT)$, in the exponent. This approach in turn requires modeling of the free energy of the growing embryos (sub-critical nuclei); in the simplest approach one can use the generic volume-plus-surface energy expressions.

Let us refer to the species (atoms, ions, molecules) which serve as monomers for the primary-particle nucleation as *solute*s. For a given concentration $c(t)$ of solutes, larger than their equilibrium saturation concentration c_0 and approaching c_0 for large times t , the rate of formation of critical nuclei can be written as [34,44]

$$\rho(t) = 4\pi a n_{cns}^{1/3} \mathcal{D} c^2 e^{-\Delta G_{cns}/kT}, \quad (7)$$

which is based on the diffusional capture of solutes, whose effective radius is denoted by a , diffusion constant by \mathcal{D} , and n is the number of solutes in an embryo. The subscript cns refers to values calculated at the critical nucleus size.

The expression (7) involves the following assumptions. For embryos of size $n < n_{cns}$, the solutes can be captured and emitted fast enough so that the size distribution is given by the equilibrium form. Thus, the factor $ce^{-\Delta G_{cns}/kT}$ in equation (7) follows from the expectation that embryo sizes up to n_{cns} are thermodynamically distributed, according the Boltzmann form. For sizes larger than n_{cns} , the dynamics is assumed to be fully ir-

reversible, corresponding to unbounded growth by capture of solutes. The factor $4\pi a n_{cns}^{1/3} \mathcal{D}c$ in equation (7) is thus the appropriate version of the Smoluchowski growth rate similar to that in equations (2) and (3). The filling-fraction correction factor was absorbed in the definition of the effective solute radius a to simplify the notation; it will be specified later.

For the free energy of formation of n -solute embryos, the following expression will be used,

$$\Delta G = -nkT \ln(c/c_0) + 4\pi a^2 n^{2/3} \sigma, \quad (8)$$

which involves the bulk term, proportional to n , and the surface term. The standard form of the bulk term was derived as follows. It is assumed that the entropic part of the free-energy change between the solid and solution phases can be calculated as the entropy in supersaturated liquid suspension of solutes of concentration c , as given by the dilute (noninteracting) expression of the “entropy of mixing,” defined, e.g., in [45]. The surface term in equation (8) corresponds to the assumption that the growing embryos are spherical, of radius $an^{1/3}$, and introduces their effective surface tension σ , which is usually assumed to be comparable to the bulk surface tension. It will be shown later that in the present case the results are very sensitive to the value of σ .

The above expressions are only meaningful for large n . It has been a common practice in the literature to use them for all n , as one of the approximations involved in a model, and treat n as a continuous nonnegative variable. Both n_{cns} and ΔG_{cns} are *explicit functions* of $c(t)$,

$$n_{cns} = \left[\frac{8\pi a^2 \sigma}{3kT \ln(c/c_0)} \right]^3, \quad (9)$$

$$\Delta G_{cns} = \frac{256\pi^3 a^6 \sigma^3}{27(kT)^2 [\ln(c/c_0)]^2}, \quad (10)$$

where the critical value n_{cns} was calculated from $\partial G/\partial n = 0$.

Next, we account for the decrease in the concentration of solutes owing to the formation of critical nuclei. Ordinarily, for $n > n_{cns}$ the primary particles grow (age) largely by absorbing diffusing solutes, and as in the preceding section we ignore here more complicated processes such as capture of small embryos, dissolution, etc. Simultaneously, the primary particles are also captured by the secondary particles. In the present model, it is assumed for simplicity that the primary particles are captured fast enough by the growing secondary particles so that the effect of their aging on the concentration of solutes can be ignored. Furthermore, it has been generally recognized that aging, when significant, tends to sharpen the size distribution [21,34]. Thus, the singlet radius r , introduced in the preceding section, will be assumed to have a unique, experimentally determined value, although in reality [1] primary particles have a peaked but finite-width size distribution. This approximation was already commented on earlier; it works largely because only the product rD matters in the rates in equations (1) through (3).

Thus, we write

$$\frac{dc}{dt} = -n_{cns}\rho(t), \quad (11)$$

which means that the concentration of solutes is “lost” solely due to the irreversible formation of the critical-size nuclei. Collecting all the above expressions, one gets the following equations for $c(t)$ and $\rho(t)$,

$$\frac{dc}{dt} = -\frac{16384\pi^5 a^9 \sigma^4 \mathcal{D} c^2}{81(kT)^4 [\ln(c/c_0)]^4} \exp\left\{-\frac{256\pi^3 a^6 \sigma^3}{27(kT)^3 [\ln(c/c_0)]^2}\right\}, \quad (12)$$

$$\rho(t) = \frac{32\pi^2 a^3 \sigma \mathcal{D} c^2}{3kT \ln(c/c_0)} \exp\left\{-\frac{256\pi^3 a^6 \sigma^3}{27(kT)^3 [\ln(c/c_0)]^2}\right\}. \quad (13)$$

It should be noted that replacing the distribution of the primary particle sizes by a single, experimentally measured average value of r , and ignoring their growth (aging) after they achieve the critical size but before they are captured, violates the conservation of matter. Thus, *in the present model only the shape of the secondary particle size distribution is relevant.* The absolute number densities N_s must be rescaled to correspond to the actual amount of solid matter per unit volume. The latter data are usually available experimentally.

4. COMPARISON WITH AN EXPERIMENT

In order to test the model developed in Sections 2 and 3, we used experimental data on the growth of dispersions of submicron spherical gold particles [1,7], which were produced by the reduction of chloroauric acid (HAuCl_4) with ascorbic acid. The simplicity of this system and possibility to either measure or estimate all the necessary parameters make it ideally suited for testing the theoretical model.

The precipitation procedure used in [1,7] has resulted in spherical gold particles of a narrow size distribution. After a short induction period (up to 6-8 sec) nucleation occurs, followed by aggregation. The total process time varies from 3 to 20 sec, depending on the experimental conditions selected. Scanning electron micrographs of the resulting particles can be seen in [1,7].

The field emission microscopy [1,7] revealed the presence of the subunits, having an approximate size of 30 to 40 nm. The calculated value for the packing fraction of the subunits in the aggregated secondary particles was characteristic of a random loose packing, usually expected in the formation of rapidly assembled systems [36]. The size of the primary particles was estimated from X-ray diffraction measurements. Calculations have generated values between 30 and 42 nm, which were in excellent agreement with the subunit size data from electron microscopy. Information on the size distribution of the primary particles is also available [1,7].

The testing of the model was carried out for a randomly selected set of experimental parameters. However, we actually varied *numerically* all the parameter values and found that the calculation results are affected to various degree by them. The parameter values will be discussed roughly in the order of increasing sensitivity of the numerical results.

The radius of the primary particles,

$$r = 2.10 \cdot 10^{-8} \text{ m}, \quad (14)$$

was obtained experimentally, as described in the preceding section, which is within the range of $0.5 \cdot 10^{-8}$ m to $5 \cdot 10^{-8}$ m, typical for the system under consideration. The value in equation (14) was for the experiment [1] for which the initial concentration was

$$c(0) = 6.0 \cdot 10^{25} \text{ m}^{-3}, \quad (15)$$

calculated from the concentration of the gold solution used in the preparation of the dispersion. The diffusion constant D of the primary particles was obtained from the Einstein formula,

$$D = 1.03 \cdot 10^{-11} \text{ m}^2 \text{ sec}^{-1}, \quad (16)$$

with

$$kT = 4.04 \cdot 10^{-21} \text{ J}. \quad (17)$$

The saturation concentration of gold in solution, c_0 , is not well known and is expected to depend somewhat on the experimental conditions. Using $2 \cdot 10^{-12}$ mol dm $^{-3}$ [46] yields

$$c_0 \simeq 1 \cdot 10^{15} \text{ m}^{-3}. \quad (18)$$

The results for the particle size distribution are not particularly sensitive to this parameter, because it enters under logarithm in equations (12)-(13). The solute diffusion constant,

$$\mathcal{D} = 1.5 \cdot 10^{-9} \text{ m}^2 \text{ sec}^{-1}, \quad (19)$$

was estimated similarly to D in equation (16), using the Einstein formula, with the radius of the gold atom of $1.44 \cdot 10^{-10}$ m [47,48]. The applicability of this formula to single atoms may not be exact, but the particle size distribution is not too sensitive to this parameter value: a decrease in \mathcal{D} shifts the calculated distribution to somewhat smaller aggregate sizes.

It was established numerically that the size distribution of the secondary particles was sensitive to the values of a , the effective atomic (solute) radius, and to the surface tension σ . Note that a was defined to relate the number of solutes n in a growing primary particle to its radius, given by $an^{1/3}$. It is assumed that the primary particles are largely crystalline; thus, the best choice of a is such that $4\pi a^3/3$ is the volume per atom, including the attributable part of the surrounding void volume, in bulk gold. Consequently,

$$a = 1.59 \cdot 10^{-10} \text{ m} \quad (20)$$

was obtained by dividing the radius of the gold atom ($1.44 \cdot 10^{-10}$ m) by the cubic root of the volume filling fraction, 0.74, of the crystalline structure of gold [36].

The effective surface tension of nanosize gold embryos in solution, σ , profoundly affects the numerical results. The bulk-gold value, which is in the range

$$\sigma \simeq 0.58 \text{ to } 1.02 \text{ N/m}, \quad (21)$$

is not known with high precision [49], and it may differ from that of the nanosize solids. Given this fact, σ was chosen as the only adjustable parameter in the model.

Experimentally, the time scale on which the secondary particle growth

effectively terminated was about 8 to 10 sec, which does not include the “induction” stage. In Figures 2 through 4, the results of the numerical simulations of the kinetic equations are presented with parameters as specified above, for three different values of σ , which clearly demonstrate the sensitivity to the choice of this parameter. In Figure 2, the case $\sigma = 0.51 \text{ N/m}$ illustrates growth that already reached saturation for times up to 10 sec. It should be noted that the distribution evolves quite slowly with time. Initially, it is heavily weighed in the small-aggregate regime. Later on, the large-size peak develops and eventually dominates the distribution. By varying σ near the expected range, given in equation (21), it was found that, for times up to 10 sec, *all* σ values yielded smaller average sizes than the experimentally measured one,

$$(R_s)_{\text{average (experimental)}} = 1.0 \pm 0.1 \mu\text{m}. \quad (22)$$

Seeking σ that would give the largest secondary particle size resulted in

$$(\sigma)_{\text{fitted}} = 0.57 \pm 0.04 \text{ N/m}, \quad (23)$$

which agrees well with the bulk value in equation (21).

Figure 3 shows the size distribution for $\sigma = 0.57 \text{ N/m}$. The growth did not reach the full saturation at the relevant times, and the peak particle radius at $t = 10 \text{ sec}$, of $R_s \simeq 0.32 \mu\text{m}$, is smaller than the experimental value in equation (22). The width of the distribution, of $\sim 10\%$, is close to that established experimentally. Given the approximations involved in the model, only semiquantitative agreement with the experimental data should be expected. Since the key feature of the model is the prediction of the narrow-width distribution of secondary particle sizes, the overall consistency with the experimental results is gratifying.

As the value of σ is increased, the large-size peak does not fully develop on the relevant time scales, as exemplified by the case $\sigma = 0.63 \text{ N/m}$ shown in Figure 4. The reader should be reminded that, owing to the absence of conservation of matter in this model, the number densities N_s must be rescaled according to the actual amount of the solid matter per unit volume, if the comparison of the calculated and experimental distributions is attempted.

Asymptotically, the particle-size distribution “freezes” for large times, i.e., the particle growth actually stops in this model as opposed to the self-similar growth studied, for instance, in [37]. Equation (11), with (9), can be integrated in closed form to yield

$$\int_0^t \rho(t') dt' = \left(\frac{3kT}{8\pi a^2 \sigma} \right)^3 c_0 \left[F \left(\frac{c(0)}{c_0} \right) - F \left(\frac{c(t)}{c_0} \right) \right], \quad (24)$$

where

$$\frac{F(x)}{x} = (\ln x)^3 - 3(\ln x)^2 + 6(\ln x) - 6. \quad (25)$$

The left-hand side of equation (24) is the total number of primary particles produced by the time t . From equations (24)-(25), this number is finite as $t \rightarrow \infty$, when $c(t) \rightarrow c_0$. The supply of primary particles, manifested by the peak at small sizes for short times, in Figures 2-4, is essential for the large-size peak in the distribution to develop and grow, because the present model assumes the growth of the secondary particles to be solely by singlet capture.

Let us consider the quantity τ defined [1] by

$$\tau = \int_0^t N_1(t') dt'. \quad (26)$$

If the independent variable is changed from t to τ in equations (1)-(4), the resulting relations are linear in $N_{s>1}$. One can establish that the only way to have a normalizable stationary size-distribution as $t \rightarrow \infty$ is to have $\tau(t)$ approach a *finite* value for large t . This quantity was calculated numerically for the σ values used in Figures 2-4. The results, shown in Figure 5, confirm the earlier observation that the growth process saturates fast for $\sigma = 0.51 \text{ N/m}$. For the two larger σ values there is still some variation for the time scales of order 1 to 10 sec; see Figure 5. The function $\tau(t)$ is useful in identifying the time scales of the growth process.

In summary, we reviewed a new model explaining synthesis of submicron size polycrystalline colloid particles with the size distribution that is narrowly peaked at an average value corresponding to a large number of primary particles in a final secondary particle. For the experimental gold-sol system the model has worked reasonably well: the average size, the width of the distribution, the time scale of the process, and even the fitted effective surface tension were all semiquantitatively consistent with the measured or expected values. The present model has involved several simplifying assumptions. Future studies will incorporate additional effects in the model and test it for a wider range of experimental systems. The main conclusion has been that multistage growth models can yield size-selection as a kinetic phenomenon, which has been observed in a large number of experimental systems.

REFERENCES

1. Privman, V., Goia, D. V., Park, J., and Matijević, E. 1999, *J. Colloid Interf. Sci.* **213**, 36.
2. Matijević, E. 1985, *Ann. Rev. Mater. Sci.* **15**, 483.
3. Haruta, M., and Delmon, B. 1986, *J. Chim. Phys.* **83**, 859.
4. Sugimoto, T. 1987, *Adv. Colloid Interf. Sci.* **28**, 65.
5. Sugimoto, T. 1982, *J. Colloid Interf. Sci.* **150**, 208.
6. Matijević, E. 1994, *Langmuir* **10**, 8.
7. Goia, D. V., and Matijević, E. 1999, *Colloids Surf.* **146**, 139.
8. LaMer, V. K. 1952, *Ind. Eng. Chem.* **44**, 1270.
9. LaMer, V. K., and Dinegar, R. H. 1950, *J. Amer. Chem. Soc.* **72**, 4847.
10. Murphy-Wilhelmy, D., and Matijević, E. 1984, *J. Chem. Soc., Faraday Trans. I* **80**, 563.
11. Matijević, E., and Murphy-Wilhelmy, D. 1982, *J. Colloid Interf. Sci.* **86**, 476.
12. Matijević, E., and Scheiner, P. 1978, *J. Colloid Interf. Sci.* **63**, 509.
13. Hsu, U. P., Rönnquist, L., and Matijević, E. 1988, *Langmuir* **4**, 31.
14. Ocaña, M., and Matijević, E. 1990, *J. Mater. Res.* **5**, 1083.
15. Ocaña, M., Serna, C. J., and Matijević, E. 1995, *Colloid Polymer Sci.* **273**, 681.
16. Lee, S.-H., Her, Y.-S., and Matijević, E. 1997, *J. Colloid Interf. Sci.* **186**, 193.
17. Edelson, L. H., and Glaeser, A. M. 1988, *J. Am. Chem. Soc.* **71**, 225.
18. Bailey, J. K., Brinker, C. J., and Mecartney, M. L. 1993, *J. Colloid Interf. Sci.* **157**, 1.

19. Morales, M. P., González-Carreño, T., and Serna, C. J. 1992, *J. Mater. Res.* **7**, 2538.
20. Ocaña, M., Morales, M. P., and Serna, C. J. 1995, *J. Colloid Interf. Sci.* **171**, 85.
21. Dirksen, J. A., and Ring, T. A. 1991, *Chem. Eng. Sci.* **46**, 2389.
22. Dirksen, J. A., Benjelloun, S., and Ring, T. A. 1990, *Colloid Polym. Sci.* **268**, 864.
23. Ring, T. A. 1991, *Powder Technol.* **65**, 195.
24. van Blaaderen, A., van Geest, J., and Vrij, A. 1992, *J. Colloid Interf. Sci.* **154**, 481.
25. Bogush, G. H., and Zukoski, C. F. 1991, *J. Colloid Interf. Sci.* **142**, 1 and 19.
26. Lee, K., Look, J.-L., Harris, M. T., and McCormick, A. V. 1997, *J. Colloid Interf. Sci.* **194**, 78.
27. Look, J.-L., Bogush, G. H., and Zukoski, C. F. 1990, *Faraday Discuss. Chem. Soc.* **90**, 345 and 377.
28. Randolph, A. D., and Larson, M. A. 1988, "Theory of Particulate Processes" (Academic Press, San Diego).
29. Brinker, C. J., and Scherer, G. W. 1990, "Sol-Gel Science" (Academic Press, Boston).
30. Flagan, R. C. 1988, *Ceramic Trans.* **1** (A), 229.
31. Scott, W. T. 1968, *J. Atmospheric Sci.* **25**, 54.
32. Higashitani, K. 1979, *J. Chem. Eng. Japan* **12**, 460.
33. Ludwig, F.-P., and Schmelzer, J. 1996, *J. Colloid Interf. Sci.* **181**, 503.
34. Overbeek, J. Th. G. 1982, *Adv. Colloid Interf. Sci.* **15**, 251.
35. Weiss, G. H. 1986, *J. Statist. Phys.* **42**, 3.

36. German, R. M. 1989, “Particle Packing Characteristics” (Metal Powder Industries Federation, Princeton).
37. Brilliantov, N. V., and Krapivsky, P. L. 1991, *J. Phys. A* **24**, 4787.
38. Krug, J., and Spohn, H. 1991, in “Solids Far from Equilibrium,” edited by Godrech  , C. (Cambridge University Press).
39. Family, F., and Vicsek, T. 1991, “Dynamics of Fractal Surfaces” (World Scientific, Singapore).
40. Medina, E., Hwa, T., Kardar, M., and Zhang, Y.-C. 1989, *Phys. Rev. A* **39**, 3053.
41. Schaefer, D. W., Martin, J. E., Wiltzius, P., and Cannell, D. S. 1984, *Phys. Rev. Lett.* **52**, 2371.
42. Reiss, H. 1951, *J. Chem. Phys.* **19**, 482.
43. Mozyrsky, D., and Privman, V. 1999, *J. Chem. Phys.* **110**, 9254.
44. Kelton, K. F., Greer, A. L., and Thompson, C. V. 1983, *J. Chem. Phys.* **79**, 6261.
45. Reif, F. 1965, “Fundamentals of Statistical and Thermal Physics” (McGraw-Hill, New York).
46. Linke, W. F. 1958, “Solubilities of Inorganic and Metal-Organic Compounds,” 4th ed., Vol. 1, p. 243 (Van Nostrand, Princeton).
47. Cotton, F. A., Wilkinson, G. and Gauss, P. L. 1995, “Basic Inorganic Chemistry,” 3rd ed., p. 61 (Wiley, New York).
48. “Gmelins Handbuch der Anorganischen Chemie,” 1954, 8th ed., p. 429 (Verlag Chemie, Weinheim).
49. “American Institute of Physics Handbook” 1957, edited by Gray, D. E., 3rd ed., p. 2-208.

FIGURE CAPTIONS

Figure 1: The two-stage growth process.

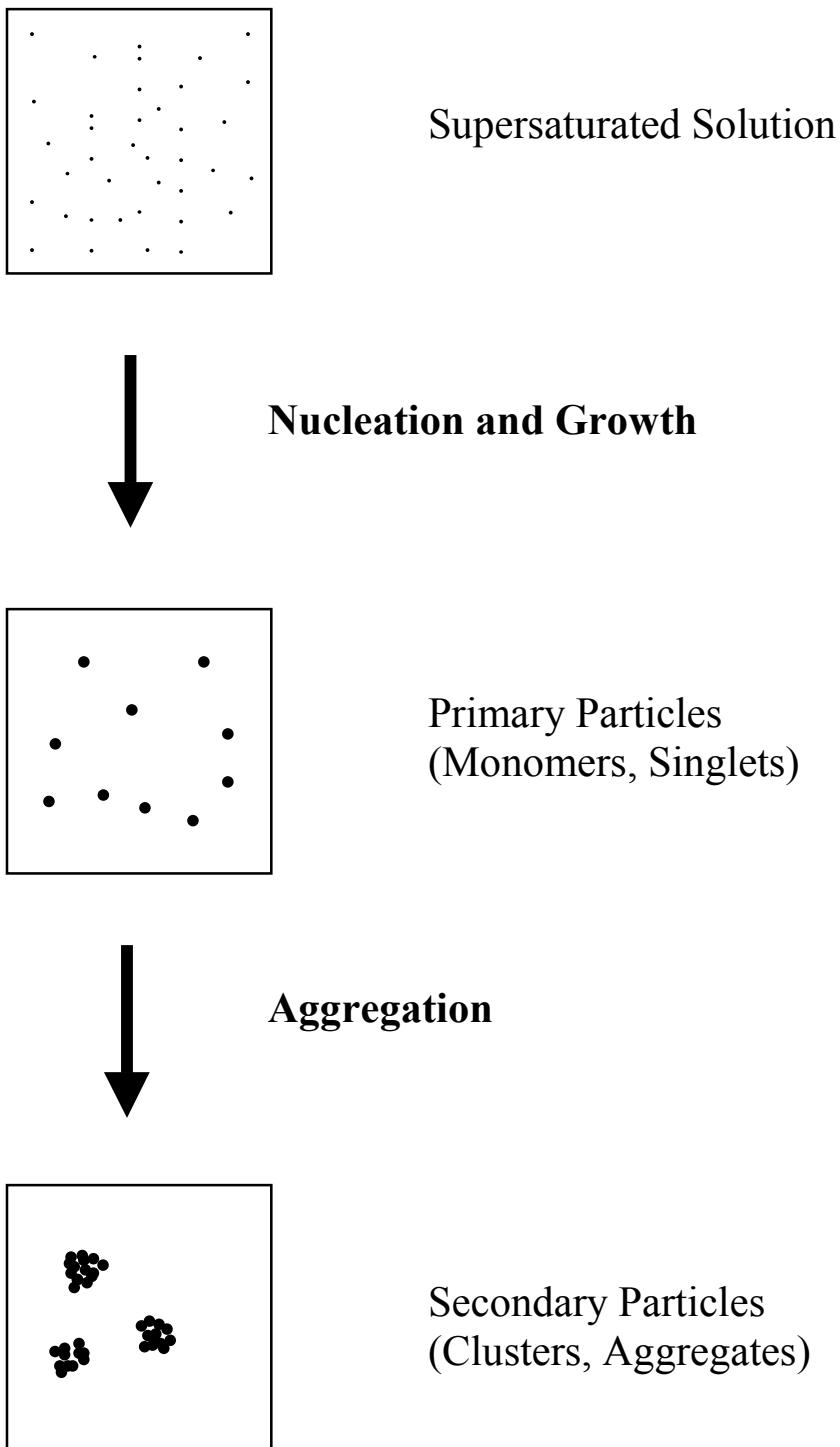
Figure 2: Distribution of secondary particles by their sizes, calculated for times $t = 0.001, 0.01, 0.1, 1, 10$ sec, using $\sigma = 0.51 \text{ N/m}$.

Figure 3: The same plot as in Figure 2, using $\sigma = 0.57 \text{ N/m}$, for times $t = 0.1, 1, 10$ sec.

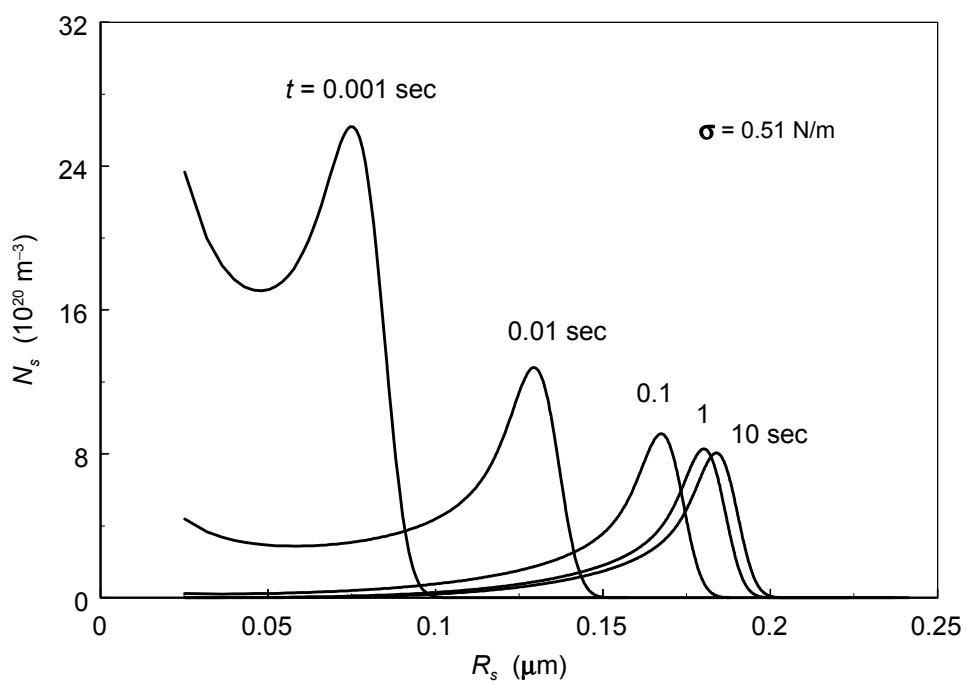
Figure 4: The same plot as in Figure 2, using $\sigma = 0.63 \text{ N/m}$, for times $t = 0.1, 1, 10$ sec.

Figure 5: The function $\tau(t)$ calculated for the values of σ corresponding to Figures 2-4.

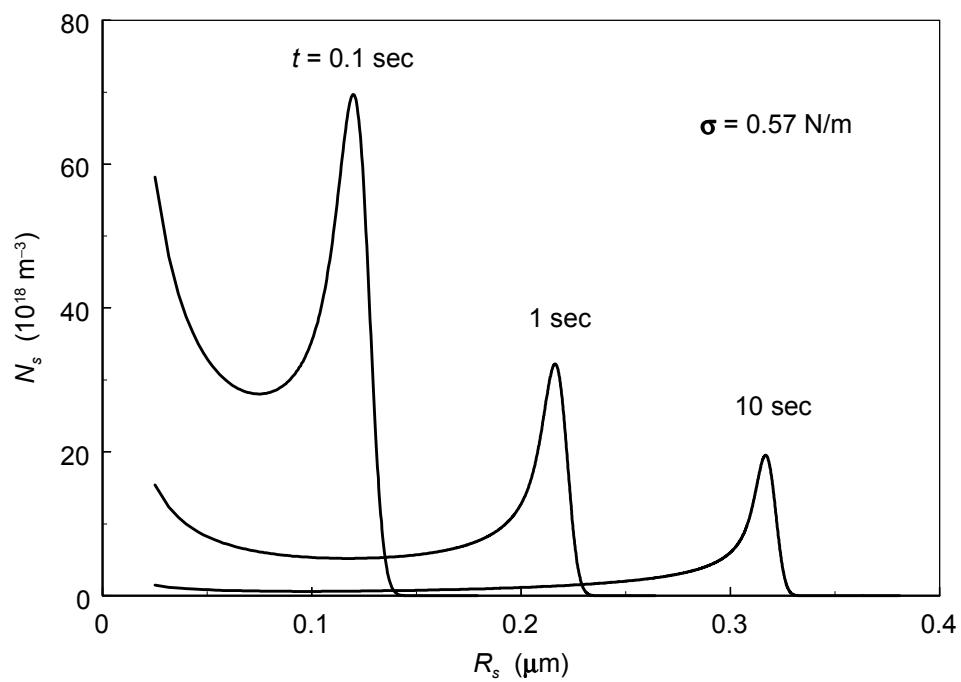
V. Privman, Figure 1



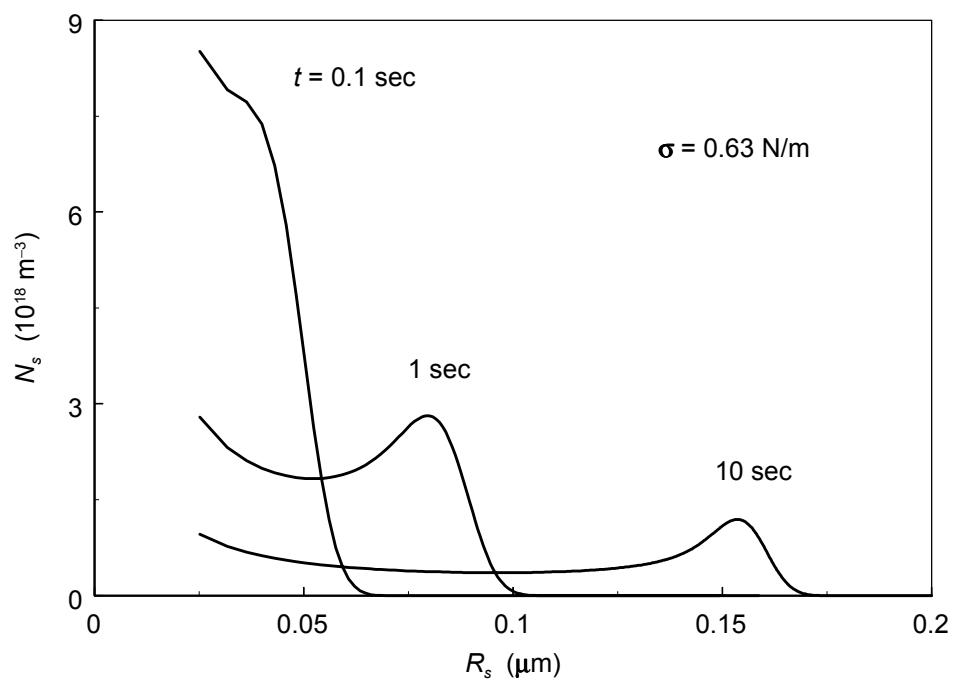
V. Privman, Figure 2



V. Privman, Figure 3



V. Privman, Figure 4



V. Privman, Figure 5

